Spin Filtering in a Hybrid Ferromagnetic-Semiconductor Microstructure

J. Wróbel,[1] T. Dietl,[2] A. Łusakowski,[1] G. Grabecki,[1] K. Fronc,[1] R. Hey,[3] K. H. Ploog,[3] and H. Shtrikman[4]

[1]*Institute of Physics, Polish Academy of Sciences, al Lotników 32/46, 02-668 Warszawa, Poland*
[2]*ERATO Semiconductor Spintronics Project, Japan Science and Technology Agency, al Lotników 32/46, 02-668 Warszawa, Poland*
[3]*Paul Drude Institute of Solid State Electronics, Hausvogteiplatz 5-7, D-10117 Berlin, Germany*
[4]*Center for Submicron Research, Weizmann Institute of Science, Rehovot 76100, Israel*

We fabricated a hybrid structure in which cobalt and permalloy micromagnets produce a local in-plane spin-dependent potential barrier for high-mobility electrons at the GaAs/AlGaAs interface. Spin effects are observed in ballistic transport in the range of tens of mT of the external field and are attributed to switching between Zeeman and Stern-Gerlach modes—the former dominating at low electron densities.

Long spin coherence times in semiconductors have triggered considerable efforts towards developing devices, in which functionalities would involve spin degrees of freedom [1]. An important building block of such devices is a spin filter, which could serve for either generating or detecting spin-polarized currents, and, indeed, spin filtering capabilities of quantum point contacts [2,3] and quantum dots [4–6] have recently been demonstrated. In those devices, a spin-dependent barrier occurs as a result of the Zeeman spin splitting generated by a strong uniform *external* magnetic field. Also the Stern-Gerlach (SG) effect has been theoretically considered as a possible spin filter in spin-logic processors [7]. There are, however, fundamental arguments against the occurrence of the SG effect for beams of electrons [8], a problem that attracts persistent attention [9–11]. At the same time, the progress in fabrication of hybrid ferromagnet-semiconductor microstructures [12,13] has made it possible to address various aspects of electron transport in the presence of an inhomogeneous magnetic field [14–19]. For example, the present authors have proposed a way to achieve spin separation by using a Stern-Gerlach apparatus for the conduction electrons residing in a quantum well and exposed to a gradient of the in-plane magnetic field [18].

In this Letter, we report on the effect of a *local* in-plane magnetic field on ballistic currents in a quantum wire patterned of a GaAs/AlGaAs heterostructure. The results are obtained for a ferromagnet-semiconductor hybrid device which is highly optimized in order to toggle between Zeeman-like (uniform field) and Stern-Gerlach–like (field-gradient) internal spin barriers. By comparing our findings to the results of conductance computations by the recursive Green-function method, we find out that the Zeeman effect dominates, particularly at low carrier densities. Owing to spin filtering and detecting capabilities that occur in a weak external magnetic field, our microstructure thus emerges as a perspective component of spintronic devices.

Figure 1(a) presents a micrograph of our device, whose design results from an elaborated optimization process

[18] and whose fabrication involves five electron-beam lithography levels, two wet-etching steps, and deposition by low-power magnetosputtering and lift-off of four different metals. A two-dimensional electron gas (2DEG) resides 95 nm below the top surface of a quantum wire of the geometrical width smoothly increasing from 0.7 to 1.4 μm, chemically etched from a modulation Si-doped (001) GaAs/(Al, Ga)As heterostructure, which was grown at the Drude Institute in Berlin. The wire is patterned along the [110] crystal axis, for which the direction of a fictitious magnetic field brought about by spin-orbit ef-
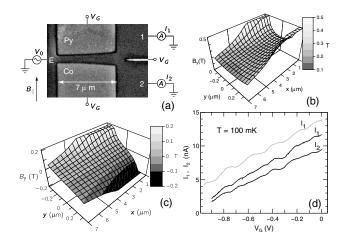

FIG. 1. (a) Scanning electron micrograph of the spin-filter device. Fixed ac voltage V_0 is applied between the emitter (E) and the "counters" (1 and 2); V_G is the dc gate voltage. The external in-plane magnetizing field ($B_\parallel$) is oriented as shown. (b) The in-plane magnetic field B_y (wider part of the channel is in front) calculated for the half-plane, 0.1 μm thick magnetic films separated by a position dependent gap $W(x)$ and magnetized in the same directions (saturation magnetization as for Co). (c) B_y calculated for antiparallel directions of micromagnet magnetizations. (d) Countercurrents I_1 and I_2 as a function of the gate voltage at $V_0 = 100$ μV and $B_\parallel = 0$; the upper curve (shown in gray) was collected during a different thermal cycle and after longer infrared illumination.

fects will be parallel to the field gradient and, therefore, will weakly affect spin dynamics [20]. The electron mobility prior to nanofabrication is $\mu = 1.76 \times 10^6$ cm^2/Vs in the dark. Hence, with the electron density $n = 2.3 \times 10^{11}$ cm^{-2}, the mean free path is of the order of the channel length. A local magnetic field is produced by NiFe (permalloy, Py) and cobalt (Co) films. The micromagnets of dimensions $40 \times 7 \times 0.1$ μm^3 reside in 0.15 ± 0.05 μm deep groves on the two sides of the wire, so that the 2DEG is approximately at the center of the field. To prevent stripe oxidation and to avoid accumulation of electrostatic charges, both micromagnets are covered with a thin (20 nm) protecting AuPd layer and connected to contact pads. An additional narrow groove patterned on the wire exit defines two regions acting as electron counters. This separating trench is filled with AuPd and also connected electrically. Annealed films of AuGe constitute Ohmic contacts between the 2DEG and current leads. The micromagnets are also used as side gates which, together with illumination by infrared radiation, serve for controlling the number of occupied 1D subbands.

We have applied Hall magnetometry in order to visualize directly the magnetizing process of the two micromagnets in question. Hall microbridges, patterned of GaAs/(Al, Ga)As : Si heterostructures grown at the Weizmann Institute in Rehovot, contain a 2DEG at 47.5 nm below the top surface on which Py and Co micromagnets, analogous to those in the spin-filter device, are deposited. Figure 2 presents Hall resistance as a function of the in-plane magnetic field $B_\parallel$ for three bridges which contain either single micromagnets or a pair of them. Steplike changes of the Hall resistance are caused by a consecutive reversal of magnetic domains. According to Fig. 2, the Co and Py micromagnets have

differing coercive fields but similar saturation magnetizations M_s. Thus, in the spin-filter device, we can compare the electric currents through the counters in the presence of the virtually uniform magnetic field (parallel magnetization directions) to the case when a strong field gradient is present. The spatial distribution of the magnetic field, evaluated under the assumption that the values of M_s correspond to that of Co, $\mu_0 M_s = 0.179$ T, are presented in Figs. 1(b) and 1(c). We see that depending on the relative magnetization directions the electrons will experience the local magnetic field B up to 0.3 T [Fig. 1(b)] or the local field gradient up to 10^6 T/m [Fig. 1(c)].

Our electron transport measurements for the spin-filter device are carried out in a dilution refrigerator at 100 mK employing a standard low-frequency lock-in technique. According to results presented in Fig. 1(d), conductance plateaus are clearly resolved. Their heights imply that the total transmission coefficient is about 0.7, a value consistent with the presence of the reflecting barrier separating the two counters. Since during these measurements micromagnets are not magnetized, a visible difference in countercurrents provides information about the degree of structure symmetry. What should we expect when the spin-dependent potential barriers are switched on? Classically, the presence of the SG effect should manifest itself by a gradient-induced symmetric enhancement of the current through both counters at given emitter-counter and gate voltages.

As shown in Fig. 3, we detect a current increase in both counters when a field gradient is produced by an appropriate cycle of the external magnetic field. The range of magnetic fields where the enhancement is observed corresponds to the shaded bands in Fig. 2(b). Furthermore, the magnitude of the stray field produced by Py is seen in
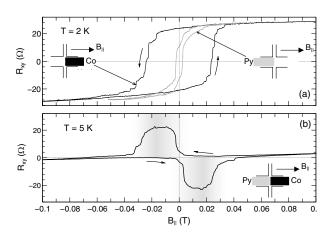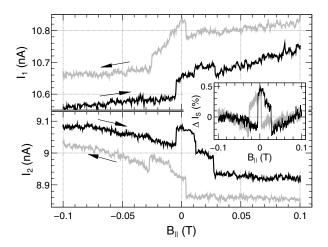

FIG. 2. Hall resistance as a function of an in-plane magnetic field measured for devices with single Co magnet and a single Py magnet (a) and with two magnets separated by a 1 μm gap (b). The arrows indicate the directions of the magnetic field sweep. Shaded bands in (b) denote the magnetic field range where the magnetizations of Co and Py micromagnets are antiparallel.

FIG. 3. I_1 and I_2 as a function of $B_\parallel$ ($V_G = 0$, $V_0 = 100$ μV, $T = 100$ mK). The arrows indicate the directions of the magnetic field sweep. The upper curves are shifted up (by 0.05 nA) for clarity. The inset shows the relative changes of the symmetric component of the signal $I_S = (I_1 + I_2)/2$, which eliminates the Hall effect, $\Delta I_S = (I_S - I_S^{++})/I_S^{++}$, where $I_S^{++} = I_S(B_\parallel = 0.1$ T).

Fig. 2(a) to diminish almost twofold prior to a change in the direction of the external magnetic field. This effect, associated with the formation of closure domains in soft magnets, explains why the current changes appear before the field reversal. The current enhancement in question is superimposed on a slowly varying background which exhibits antisymmetric behavior for the two counters. We assign its presence to a residual effect of the Lorentz force (Hall effect) associated with a possible misalignment of the micromagnets in respect to the 2DEG plane.

We checked that results presented in Fig. 3 are unaltered by increasing the temperature up to 200 mK and independent of the magnetic field sweep rate. The relative change ΔI of countercurrent depends, however, on V_G, where I is either I_1 or I_2. Figure 4 shows I_1 vs $B_\parallel$ for several values of V_G (I_2 behaves in the same manner). $\Delta I/I$ increases from 0.5% at zero gate voltage to 50% close to the threshold. Furthermore, for V_G about -0.8 V ΔI is negative.

We evaluate the expected magnitude of $\Delta I/I$ within the model of quantum ballistic transport, which we developed previously [20] by employing the recursive Green-function method. We note that the key feature of our experimental configuration is a dramatic reduction of the influence of the Lorentz force by electron confinement. In particular, the effect of the in-plane magnetic field $B_{x,y}$ is much reduced by the interfacial electric field and by the corresponding quantization of electron motion in the z direction. Furthermore, since a residual field B_z brought about by misalignment of the magnet centers tends to vanish in the branching region, its influence on electron dynamics will be small [21], in agreement with a weak asymmetry of data in Figs. 3 and 4. Under these assumptions, electron dynamics is governed by the potential $V(x, y)$ determined by the device geometry, taken in the form corresponding to Fig. 1(a) as well as by the Pauli term, $g^* sB$, where $B = [0, B_y(x, y), 0]$ with $B_y(x, y)$ displayed in Figs. 1(b) and 1(c) for both magnetization configurations. Because of the low density of electrons in the quantum wire, we expect a considerable enhance-
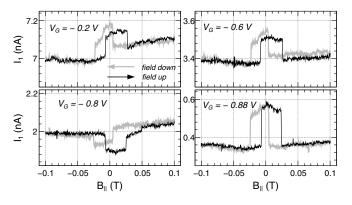
ment of the electron Landé factor. The interaction induced renormalization of the g factor has already been observed experimentally for the gated low-density 2D electron gas [22,23]. While the role of many body effects in confined systems is under an active debate presently, we take their existence into account by allowing for an enhancement of the Landé factor to the value $|g^*| = 2.0$.

The computed conductance G_0 of our model device is shown in Fig. 5(a) as a function of the electrostatic potential barrier height. Black and gray lines correspond to the Zeeman-like and Stern-Gerlach–like spin-dependent barriers, respectively. As expected, when both micromagnets are polarized in the same direction an additional spin-resolved narrow plateau shows up. Reversing the magnetization of the Py pole while leaving the Co pole unaffected corresponds to the transition from the black to the gray curve. As a result, at the transition region between plateau ΔG_0 is either positive or negative. At the quantized plateau, the conductance does not depend on the type of the spin barrier, and the spatial distribution of *total* current density is only slightly modified by the presence of the field gradient. Under these conditions, however, the spatial separation of the potential wells for the particular spin directions makes the electric current at opposite edges of the device to be strongly "left" or "right" spin polarized, up to 50% for $G_0 = 1$. This indicates that the SG effect is present under our experimental conditions though it contributes weakly to the current enhancement visible in Figs. 3 and 4.

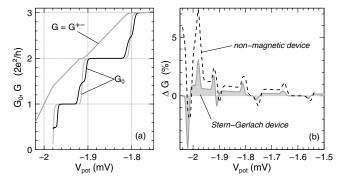It is clear that G_0 should be averaged over a nonzero energy window corresponding to the applied

FIG. 5. (a) G_0 and G calculated for parallel (black) and antiparallel (gray) magnetizations. G is computed taking into account the presence of nonzero bias $V_0 = 100$ μV; G^{+-} corresponds to the Stern-Gerlach configuration. The hard wall model potential $V(x, y)$ and minimal channel width $W_0 = 0.5$ μm are used. An additional electrostatic potential V_{pot} is adiabatically introduced to simulate the gate voltage [24], the separating groove is not modeled, and scattering is absent. Conductances are shown as a function of V_{pot} for electron energy $E = 2$ meV. (b) Relative changes of the conductance ΔG. Solid line: $\Delta G = (G^{+-} - G^{++})/\langle G \rangle$, where G^{++} corresponds to the spin-filter configuration; $\langle G \rangle$ is the mean value. Dashed line: $\Delta G = [G(B_\parallel = 0) - G(B_\parallel = 0.3$ T)$]/\langle G \rangle$ for the nonmagnetic device.

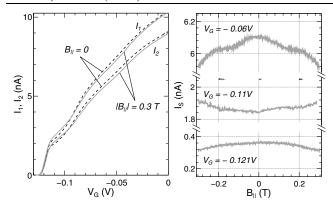FIG. 4. The countercurrent I_1 as a function of the in-plane magnetic field for various gate voltages.

FIG. 6.   Countercurrents I_1, I_2, and $I_S = (I_1 + I_2)/2$ at bias $V_0 = 100$ μV and at 100 mK as a function of the gate voltage (left) and in-plane magnetic field (right), for the *nonmagnetic* device. The width of channel was slightly narrower and the pinch-off voltage was smaller than for the "magnetic" structure.

emitter/counter voltage. We defined the observed conductance as $G = \int_{\mu_1}^{\mu_2} G_0(E)dE$, where E is the electron energy and $\mu_2 - \mu_1 = eV_0$. The averaging procedure narrows the plateaus, but quite remarkably, the nonzero bias ($V_0 = 100$ μV), which is ~3 times larger than the expected spin splitting (30 μeV for $g^* = 2$), does not smear out the changes of the conductance associated with the presence of the Zeeman barrier. Actually, it extends the regions of conductance changes towards the quantized plateaus of G_0. We see that the computed magnitude of the effect compares favorably with the experimental findings. Except for the immediate vicinity of the pinch-off region, our model describes the magnitude of the current changes and explains why the sign of the effect can be negative for some values of V_G.

According to the above interpretation, similar gate-voltage dependent current changes should be generated by a Zeeman barrier produced by an external in-plane magnetic field of the magnitude comparable to the stray fields of the micromagnets. To test this expectation we fabricated a nonmagnetic version of our device, in which both magnets were replaced by the AuPd gates of the approximately same size. Figure 6 shows I_1, I_2, and $I_S = (I_1 + I_2)/2$ as a function of $B_{\parallel}$ and V_G. The character and magnitude of these changes is compatible with theoretical expectations depicted by the dashed line in Fig. 5(b), which supports strongly our model. However, in contrast to the SG device, no enhancement of the effect is observed near the pinch-off. This may suggest a nontrivial influence of the field gradient on spin transport in this regime or a modification of the pinch-off voltage by magnetization-dependent strains.

In conclusion, the experimental and theoretical study presented here demonstrates that semiconductor nanostructures of the kind proposed in this work can serve to generate and detect spin-polarized currents in the absence of an external magnetic field. Moreover, according to our results, the degree and direction of spin polarization at low electron densities can easily be manipulated by gate voltage or a weak external magnetic field. While the results of our computations suggest that the spin separation and thus the Stern-Gerlach effect occurs under our experimental conditions, its direct experimental observation would require incorporation of spatially resolved spin detection.

[1] *Semiconductor Spintronics and Quantum Computation*, edited by D. D. Awschalom, D. Loss, and N. Samarth (Springer-Verlag, Berlin, 2002).
[2] R. M. Potok *et al.*, Phys. Rev. Lett. **89**, 266602 (2002).
[3] G. Grabecki *et al.*, Physica (Amsterdam) **13E**, 649 (2002).
[4] J. A. Folk *et al.*, Science **299**, 679 (2003).
[5] M. Ciorga *et al.*, Appl. Phys. Lett. **80**, 2177 (2002).
[6] R. Hanson *et al.*, cond-mat/0311414 [Phys. Rev. B (to be published)].
[7] C. H. W. Barnes, J. M. Shilton, and A. M. Robinson, Phys. Rev. B **62**, 8410 (2000).
[8] N. F. Mott, Proc. R. Soc. London A **124**, 425 (1929).
[9] H. Batelaan, T. J. Gay, and J. J. Schwendimann, Phys. Rev. Lett. **79**, 4517 (1997).
[10] B. M. Garraway and S. Stenholm, Phys. Rev. A **60**, 63 (1999).
[11] G. A. Gallup, H. Batelaanm, and T. J. Gay, Phys. Rev. Lett. **86**, 4508 (2001).
[12] M. Johnson *et al.*, Appl. Phys. Lett. **71**, 974 (1997).
[13] T. Matsuyama *et al.*, Phys. Rev. B **65**, 155322 (2002).
[14] G. Grabecki *et al.*, Physica (Amsterdam) **21E**, 451 (2004).
[15] A. Nogaret, S. J. Bending, and M. Henini, Phys. Rev. Lett. **84**, 2231 (2000).
[16] D. N. Lawton *et al.*, Phys. Rev. B **64**, 033312 (2001).
[17] S. M. Badalyan and F. M. Peeters, Phys. Rev. B **64**, 155303 (2001).
[18] J. Wróbel *et al.*, Physica (Amsterdam) **10E**, 91 (2001).
[19] J. Fabian and S. Das Sarma, Phys. Rev. B **66**, 024436 (2001).
[20] A. Łusakowski, J. Wróbel, and T. Dietl, Phys. Rev. B **68**, 081201(R) (2003).
[21] C. W. J. Beenakker and H. van Houten, Phys. Rev. Lett. **63**, 1857 (1989).
[22] J. Zhu *et al.*, Phys. Rev. Lett. **90**, 056805 (2001).
[23] E. Tutuc, S. Melinte, and M. Shayegan, Phys. Rev. Lett. **88**, 036805 (2002).
[24] eV_{pot} is the electrostatic barrier induced by V_G. To find the relation between V_{pot} and V_G a self-consistent modeling is needed; see, e.g., G. L. Snider, I.-H. Tan, and E. L. Hu, J. Appl. Phys. **68**, 2849 (1990).